Article

On the Efficacy of a Novel Optimized Tuned Mass Damper for Minimizing Dynamic Responses of Cantilever Beams

Baki Ozturk [1], Huseyin Cetin [2], Maciej Dutkiewicz [3], Ersin Aydin [4] and Ehsan Noroozinejad Farsangi [5,*]

[1] Department of Civil Engineering, Hacettepe University, Ankara 06800, Turkey
[2] Department of Construction Technology, Nigde Omer Halisdemir University, Nigde 51100, Turkey
[3] Faculty of Civil, Architecture and Environmental Engineering, University of Science and Technology in Bydgoszcz, 85-796 Bydgoszcz, Poland
[4] Department of Civil Engineering, Nigde Omer Halisdemir University, Nigde 51100, Turkey
[5] Faculty of Civil and Surveying Engineering, Graduate University of Advanced Technology, Kerman 7631885356, Iran
* Correspondence: noroozinejad@kgut.ac.ir

Abstract: This study examines the optimal design of a tuned mass damper (TMD) in the frequency domain so that the dynamic response of cantilever beams can be decreased. Random vibration theory is applied to identify the mean square acceleration of the endpoint of a cantilever beam as the objective function to be reduced. In addition, to determine the optimal TMD coefficient of mass, stiffness, and damping, a differential evolution (DE) optimization algorithm is employed. The upper and lower limit values of these parameters are taken into account. A majority of the previous studies have concentrated on determining just the stiffness and damping parameters of TMD. Nonetheless, in this study there is also the optimization of TMD mass parameters to determine the mass quantity. In addition, there has been inefficient use of the stochastic DE optimization algorithm method for the optimization of TMD parameters in previous studies. Hence, to obtain optimal TMD parameters, this algorithm is precisely used on the objective function. Tests are carried out on the cantilever beam with the TMD system following this optimization method with harmonic base excitations that resonate the foremost modes of the beam and white noise excitation. The method proposed here is reasonably practical and successful regarding the optimal TMD design. When a TMD is designed appropriately, the response of the cantilever beam under dynamic interactions undergoes a considerable reduction.

Keywords: cantilever beam; vibration control; tuned mass damper; transfer function; differential evolution; resilience

1. Introduction

A tuned mass damper (TMD) is a vibration absorber that includes a mass, a damper, and a spring. The spring and damper are linked to the TMD mass in this device in series, and they are connected in parallel with one another. In practice, the resonance frequency is very important for design [1]. In order to prevent resonance issues in the structures, TMD is a very useful design tool. Inertial forces are involved in the dynamic energy absorption technique of TMD when the primary system is shifted by dynamic excitation forces. This energy absorption signifies the kinetic energy absorption that attains the highest value when the phase angle between the primary structure and the TMD movements is $\pi/2$ radians. This suggests that the highest kinetic energy absorption takes place when TMD works in the direction opposite to the central structure. Here, there is an increase in the equivalent effective damping quantity due to energy dissipation when the value of the fundamental natural frequency of the main structure is close to that of the TMD frequency value [2,3].

Hermann Frahm carried out the first study of TMDs in 1909 to decrease the impact of the hazardous vibration of ship engines on the keel of ships [3]. The theoretical research

pertinent to TMDs was first carried out by Ormondroyd and Den Hartog [4]. The system regulated by TMDs was examined by Bishop and Welbourn, while maintaining the internal damping of the structure [5]. The major mass TMD system was optimized by Falcon [6], considering the internal damping of the structure. A few correction factors were included by Ioi and Ikeda [7] in the damping parameters of TMDs. A technique was proposed by Warburton and Ayorinde [8] to identify the optimal mass ratio and damping parameter of TMDs. Optimal damping of TMDs was computed by Vickery et al. [9] by taking into account the main mass with a natural damping ratio of 5%. Villaverde and Koyoama [10] examined the effectiveness of a TMD in a ten-story building in the context of the Mexico City earthquake. Soto-Brito and Ruiz [11] examined the effectiveness of a TMD for earthquake response reduction on a twenty-two-story nonlinear shear building. They reported that a TMD is effective for the response reduction in this nonlinear shear building under low and moderate intensity earthquakes. Bektas and Nigdeli [12] used the metaheuristic harmony search algorithm to find the optimal TMD parameters for seismically excited structures. In their study, the mass ratio factor of TMDs was also investigated [13]. Cetin et al. [14] proposed a method related to optimal viscous damper distribution in shear buildings controlled with TMDs. An efficient optimal TMD design technique was put forward by Cetin and Aydin [15] on the basis of the transfer function by employing a differential evolution (DE) algorithm. Takewaki [16] investigated optimal damper locations in a cantilever beam for dynamic compliance. A rotational and translational vibration absorber was suggested by Wong et al. [17] in order to isolate beam vibration, which is exposed to point or distributed excitations. Bae et al. [18] aimed to decrease the vibration in a cantilever beam by using magnetic TMD. Aly [19] proposed a tuned mass damper for response mitigation in wind-exposed structures. Moreover, it is observed that fuzzy logic and linear quadratic Gaussian controllers improve TMD performance. Zhang and Xu [20] proposed that the goal of the optimization process is to identify the minimal TMD mass required to permit the nonlinear objective.

The design ramifications of tuned mass dampers under dynamic load and uncertainty in the model are crucial. As shown in Figure 1 [21], the input energy in the frame can be significantly decreased if the input energy criterion caused by dynamic excitation holds roughly even, regardless of the existence of inherent damping of the system, and the included tuned mass damper can absorb the dynamic input energy as significantly as possible. The overall input energy applied to a single-degree-of-freedom system (SDOF) without TMD as well as an SDOF system with TMD can be seen in Figure 1 [21]. Figure 1a shows that the input energies brought about by output disruptions like wind and earthquakes are stored in the main frame. Hence, harmful destruction can possibly take place within the structure. Nevertheless, it can be seen in Figure 1b that TMD decreases the dissipated energy by frame. Hence, it is possible to avoid the significant damage to the structure.

This study examines the optimum design of a single TMD that is kept at the end node of a cantilever beam so that the translational and rotational dynamic energies can be regulated. Using random vibration theory, this research examines the best configuration for a tuned mass damper located at the end node of the cantilever beam. The cantilever–TMD system is exposed to first, second, and third mode sinusoidal harmonic and random white noise excitation. Using a differential evolution optimization approach that takes into consideration the provided restrictions, the mean-square end node of the beam acceleration and top displacement are minimized based on transfer functions. The optimization of a single-TMD (SDOF) system is less difficult than the optimization of a multi-TMD (MDOF) system. MDOF systems are often decoupled in order to become SDOF systems in conventional solutions. Only one form of control may be used, since common procedures are restricted. A more practical method would be to use TMDs to control multiple frequencies or additional control modes. It should be stated that the mass of the dampers is defined. However, in a traditional design, the mass is often set by the designer in order to determine the best stiffness and damping coefficients. In the proposed method, TMD mass quantity is optimized together with stiffness and damping. A differential evolution (DE) optimiza-

tion algorithm is used to compute the mass coefficient of TMDs, taking into account the constraints determined, while the equation of motion is included in the frequency domain. The power special density (PSD) function of external disturbance is defined in the form of white light in a given road frequency range, so that there is no restriction on the design by a given frequency. When random vibration theory is considered, the mean square of the acceleration of the end node of the cantilever beam is taken to be an objective function, and the goal is to decrease it. The rotational and translational vibration of the cantilever beam is regulated by the designed TMD. A harmonic base excitation considering the first three natural frequencies that resonate with the fundamental mode of a beam and white noise excitation, which is randomly produced, are used to test it. The results are compared to a few other frequently used methods in the literature to corroborate the findings. The findings of this study show that an appropriately designed TMD is effective in decreasing the cantilever beam's rotational as well as its translational vibrational responses.
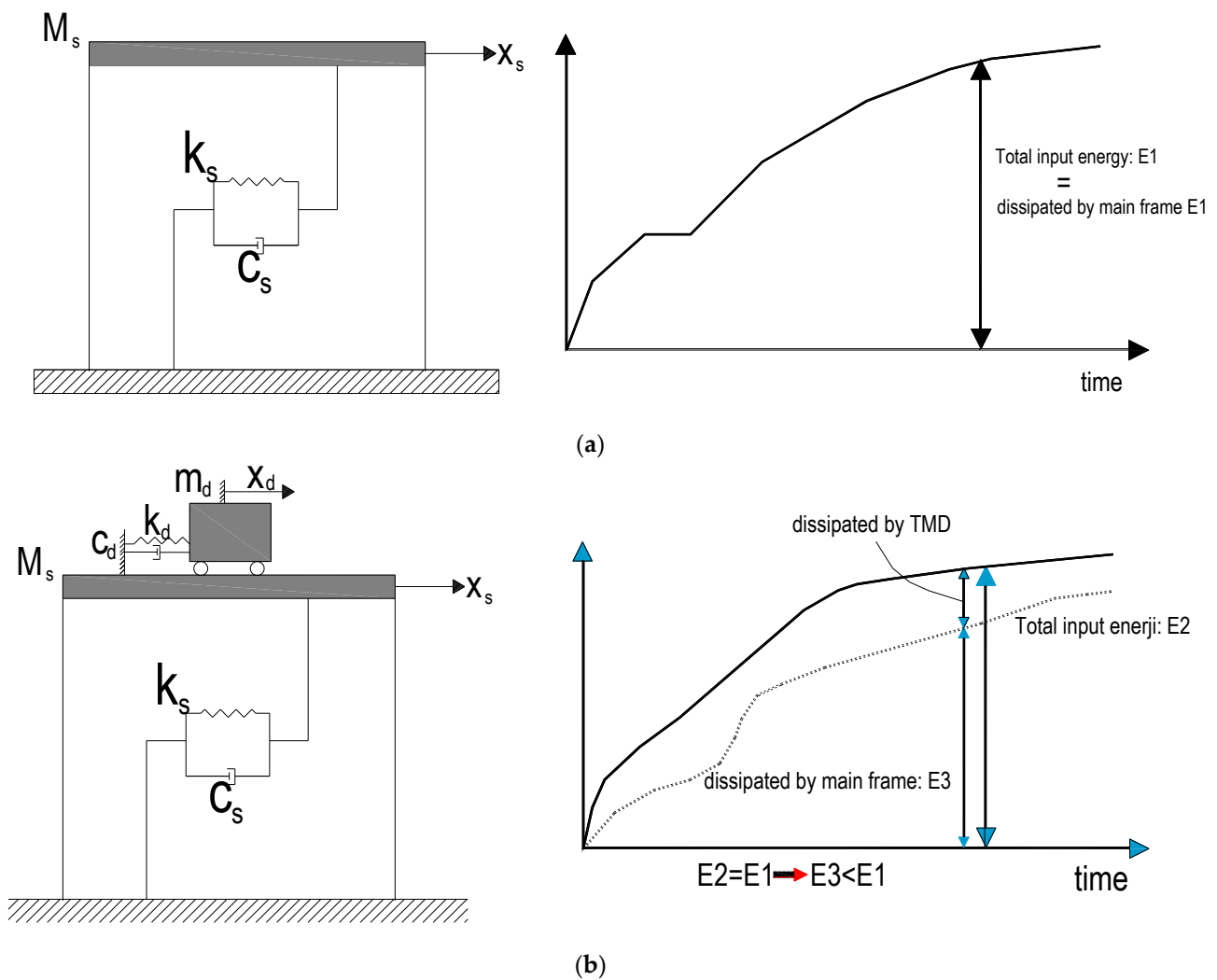
Figure 1. Total input energy applied to: (**a**) an SDF system without TMD and (**b**) an SDF system with TMD.

Section 2 of the remaining work contains information regarding the tuned mass dampers and the definition of the cantilever beam model is included. Section 4 presents a numerical example to show how successful the suggested methods are, and Section 3 describes the optimization issue and the method for the TMD design. Section 3 also provides a full analysis and interpretation of the results. Furthermore, Section 5 describes the findings of this investigation.

2. Cantilever Beam Model with Tuned Mass Dampers

Figure 2 demonstrates a typical cantilever beam with a TMD system that faces base disturbance. This figure shows that the translational and rotational displacement vectors may be described as a vector, where $x(t) = \{x_1, \theta_1, x_2, \theta_2, \dots x_{n-1}, \theta_{n-1}, x_n, \theta_n, x_{TMD}\}$ in $(2n + 1)$ dimensions. In this expression, x_n demonstrates the vertical displacement of the beam and the acceleration of the random base excitation is indicated by $\ddot{x}_{dist}(t)$. Przemieniecki [22] provides the element stiffness k and mass matrices m of the Timoshenko beam.

$$k = \frac{EI}{L^3(1+\phi)} \begin{bmatrix} 12 & 6L & -12 & 6L \\ 6L & L^2(4+\phi) & -6L & L^2(2-\phi) \\ -12 & -6L & 12 & -6L \\ 6L & L^2(2-\phi) & -6L & L^2(4+\phi) \end{bmatrix} \tag{1}$$

$$m = \frac{\rho AL}{(1+\phi)^2} \begin{bmatrix} m_1 & m_2 & m_3 & m_4 \\ m_2 & m_5 & -m_4 & m_6 \\ m_3 & -m_4 & m_1 & -m_2 \\ m_4 & m_6 & -m_2 & m_5 \end{bmatrix} + \frac{\rho AL}{(1+\phi)^2}\left(\frac{r}{L}\right)^2 \begin{bmatrix} m_7 & m_8 & -m_7 & m_8 \\ m_8 & m_9 & -m_8 & m_{10} \\ -m_7 & -m_8 & m_7 & -m_8 \\ m_8 & m_{10} & -m_8 & m_9 \end{bmatrix} \tag{2}$$

where,

$$m_1 = \frac{13}{35} + \frac{7\phi}{10} + \frac{\phi^2}{3}, \; m_2 = \left(\frac{11}{210} + \frac{11\phi}{120} + \frac{\phi^2}{24}\right)L, \; m_3 = \frac{9}{70} + \frac{3\phi}{10} + \frac{\phi^2}{6},$$

$$m_4 = -\left(\frac{13}{420} + \frac{3\phi}{40} + \frac{\phi^2}{24}\right)L, \; m_5 = \left(\frac{1}{105} + \frac{\phi}{60} + \frac{\phi^2}{120}\right)L^2, \; m_6 = -\left(\frac{1}{140} + \frac{\phi}{60} + \frac{\phi^2}{120}\right)L^2,$$

$$m_7 = \frac{6}{5}, m_8 = \left(\frac{1}{10} - \frac{\phi}{2}\right)L, m_9 = \left(\frac{2}{15} + \frac{\phi}{6} + \frac{\phi^2}{3}\right)L^2, m_{10} = \left(-\frac{1}{30} - \frac{\phi}{6} + \frac{\phi^2}{6}\right)L^2 \tag{3}$$
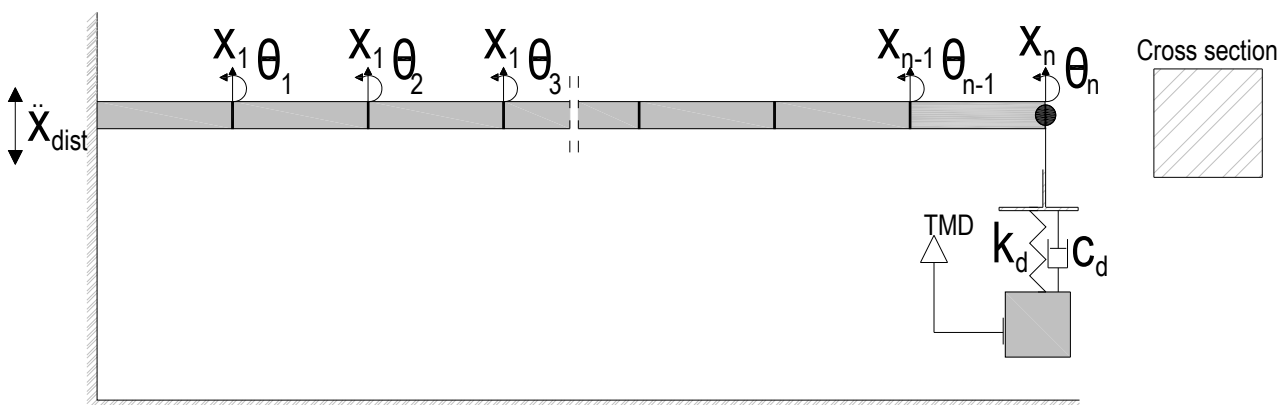
Figure 2. Cantilever beam–TMD model.

Here, $r = \left(\frac{I}{A}\right)$ and $\phi = \left(\frac{12EI}{(G\kappa AL^2)}\right)$. $E, I, G, \kappa, A, L,$ and ρ represent the modulus of elasticity, moment of inertia, shear modulus, shear correction factor, cross section area, length of the element, and mass density, respectively.

The equation of motion is presented below:

$$(M_s + M_{TMD})\, \ddot{x}(t) + (C_s + C_{TMD})\, \dot{x}(t) + (K_s + K_{TMD})\, x(t) = -(M_s + M_{TMD})r\ddot{x}_{dist}(t) \tag{4}$$

This equation shows $\ddot{x}(t)$ and $\dot{x}(t)$ as the translational and rotational acceleration and velocity vectors of the cantilever beam, respectively. The mass, damping, and stiffness matrices of the beam are signified by M_s, C_s, and K_s, respectively in $(2n + 1) \times (2n + 1)$ dimensions. The mass, damping, and stiffness matrices of the TMD are shown by M_{TMD}, C_{TMD}, and K_{TMD}, respectively. Finally, the impact of the vector in $(2n + 1)$ dimensions is represented by $r = \{1, 0, 1, 0, \dots 1\}$.

A different approach is used to describe structural damping, which is taken to be proportional to mass in this study. To achieve the transfer function of the equation of motion, the following equation can be used to show the Fourier transform of the previous equation.

$$(K + i\omega C - \omega^2 M)X(\omega) = -Mr\ddot{X}_{dist}(\omega) \tag{5}$$

In this equation, the transfer function of white noise base excitation is represented by $\ddot{X}_{dist}(\omega)$; the disturbance frequency is shown by $X(\omega)$; the Fourier transform of the displacement vector in $(2n + 1)$ dimensions is indicated by $X(\omega)$; and the mass, damping, and stiffness matrices of a cantilever beam regulated by a TMD are represented by M, C, and K, respectively. The dimensions of these matrices are $(2n + 1) \times (2n + 1)$, and $i = \sqrt{-1}$ shows the imaginary part. The reduced Equation (5) is shown as follows:

$$AX(\omega) = -Mr\ddot{X}_{dist}(\omega) \tag{6}$$

In this equation, matrix A is described as follows.

$$A = \left(K + i\omega C - \omega^2 M\right) \tag{7}$$

The following equation can be used to denote the Fourier transform of the displacement vector $X(\omega)$.

$$X(\omega) = -A^{-1}Mr\ddot{X}_{dist}(\omega) \tag{8}$$

Similarly, the Fourier transform of the acceleration is represented as:

$$\ddot{X}_{AA}(\omega) = H_{AA}(\omega)\ddot{X}_g(\omega) \tag{9}$$

where the absolute value of the acceleration transfer function $H_{AA}(\omega)$ may be expressed as

$$H_{AA}(\omega) = \left(1 + \omega^2 A^{-1} Mr\right) \tag{10}$$

$S_{dist}(\omega)$ can be denoted as the spectral density function of a stationary random process. Random vibration theory can be used to represent the mean square of the absolute acceleration σ^2_{AAi} of the ith component as follows:

$$\sigma^2_{AAi} = \int_{-\infty}^{\infty} |H_{AAi}(\omega)|^2 S_g(\omega)d\omega = \int_{-\infty}^{\infty} H_{AAi}H^*_{AAi}S_g(\omega)d\omega \tag{11}$$

In this equation, $()^*$ signifies the complex conjugate and $|H_{AAi}(\omega)|$ refers to the absolute value of the acceleration transfer function of the ith component.

3. Optimization Problem and Method for TMD Design

Taking the numerical nonlinear constrained optimization problems in engineering into account, there are many methods that are available in the literature. Basically, these optimization methods can be divided into two types. The first are gradient-based optimization algorithms that use the first and second derivatives. The second are the direct search algorithms, which do not need derivatives. Although direct search algorithms reach the solution slower than gradient-based algorithms, they are more robust against the noise in the objective function and its constraints [23].

The optimization criterion is identified by the design purpose. For example, displacement minimization improves safety and reduces deformations in the structure, while acceleration minimization prevents damage to non-structural elements. Acceleration minimization also reduces the disturbing vibration, which affects the level of comfort in the structure and reduces the base shear force.

To determine the optimal TMD parameters for the response reduction of a cantilever beam, the closed form of the statistical objective functions (f_1), which denotes the mean square of acceleration of the nth freedom of the beam and the mean square of the displacement (f_2) of the nth freedom of the beam, can be expressed as follows:

$$f_1(k_d, m_d, c_d,) = \sigma^2_{AAn} \tag{12}$$

$$f_2(k_d, m_d, c_d,) = \sigma^2_{Dn} \tag{13}$$

The following can be used to determine the optimization constraints:

$$0 \le k_d \le \bar{k}_d \tag{14}$$

$$0 \le m_d \le \bar{m}_d \tag{15}$$

$$0 \le c_d \le \bar{c}_d \tag{16}$$

The upper limits of the coefficients of TMD stiffness, mass, and damping are represented by $\bar{k}_d$, $\bar{m}_d$, and $\bar{c}_d$ in Equations (14)–(16), respectively.

4. DE Algorithm

Differential evolution is a robust, stochastic, nonlinear global optimization method [24]. Due to the comparatively large collection of points it maintains, it is reasonably resilient but typically slower than other approaches. This approach was utilized in this study to identify the best optimized tuned mass damper (TMD) design parameters because of its resilience and success for global optimization. Moreover, this method is not widely used for the optimal design of TMD for response reduction of the cantilever beam.

No optimization algorithm exists that always ensures global resolution, particularly for nonlinear, non-differentiable, and non-continuous issues. The proposed DE method is an effective and rigorous stochastic population-based algorithm that generally tries to achieve a globally optimal solution. Four fundamental steps are undertaken in evolutionary algorithms, including initialization, mutation, recombination, and selection, which are expressed as follows [25–27].

4.1. Definition of the Target Vector under the Lower and Upper Bounds and Determination of the Population Matrices

Let $\vec{X}_i^g$ be the target vector for the gth generation and i^{th} population. This vector can be expressed as

$$\vec{X}_i^g = \{x_{1,i}^g, x_{2,i}^g, \ldots, x_{D,i}^g,\}, \qquad i = 1, \ldots, \text{NP} \tag{17}$$

in which D shows the dimension of the problem (number of variables to be found) and NP is the number of populations, which can usually be chosen between $2D$ and $4D$ [28]. In this study, the stiffness, mass, and damping coefficients of TMD are the dimensions of the problems. Therefore, the number of the population (NP) can be determined between $2 \times 3 = 6$ and $4 \times 3 = 12$. For the ith population, the target vector can be determined as $x_{1,i}^g = m_{d,i}^g$, $x_{2,i}^g = c_{d,i}^g$, $x_{3,i}^g = k_{d,i}^g$ for the coefficients of the TMD.

In the beginning, the generation number g is set equal to zero. The jth dimension of the ith population of the problem can be calculated as

$$x_{ij}^0 = x_{j,Low} + rand_{i,j}(0,1). \left(x_{j,Up} - x_{j,Low}\right) \tag{18}$$

In this equation, $x_{j,Low}$, and $x_{j,Up}$ are the lower and upper bounds of the jth dimension, respecitvely. $rand_{i,j}(0,1)$ is a random real number between [0] and [1] for the ith population.

4.2. Donor Vector Creation through Mutation

Let R_1^i, R_2^i and $R_3^i \in$ [1, NP] and the donor vector $\vec{V}_i^g$ is composed of three target vectors $\vec{X}_{R_1^i}^g$, $\vec{X}_{R_2^i}^g$, and $\vec{X}_{R_3^i}^g$, which are randomly chosen for the ith population. The donor vector for the ith population of the gth generation can be written as

$$\vec{V}_i^g = \vec{X}_{R_1^i}^g + \text{F.} \left(\vec{X}_{R_2^i}^g - \vec{X}_{R_3^i}^g \right) \tag{19}$$

in which the scaling factor F is a real number between [0] and [1].

4.3. Recombination and Composing of the Test Vector

Let $\vec{u}_i^g$ be the test vector of gth generation and i^{th} population. This vector can be written as

$$\vec{u}_i^g = \{u_{1,i}^g + u_{2,i}^g + \ldots + u_{D-1,i}^g + u_{D,i}^g\} \ i = 1, \ldots, \text{NP} \tag{20}$$

The component of the test vector $u_{j,i}^g$ for the jth dimension of the ith population is determined with respect to the target vector component $x_{j,i}^g$; and the component of the donor vector $v_{j,i}^g$ can be obtained as follows.

$$u_{j,i}^g = \begin{cases} v_{j,i}^g, & if\left(rand_{i,j}(0,1) \ \leq \ C_r \ veya \ j = j_{rand} \right) \\ x_{j,i}^g, & otherwise \end{cases} \tag{21}$$

where the real number C_r is the crossing rate between [0,1]. j_{rand} is an integer number which is between [1, D].

4.4. Selection

In the selection step, the target vector function $f\left(\vec{X}_i^g\right)$ and the test vector $f\left(\vec{u}_i^g\right)$ are compared. If $f\left(\vec{u}_i^g\right) \leq f\left(\vec{X}_i^g\right)$, the selection is the donor vector $\vec{u}_i^g$, therefore the optimum solution is obtained. Otherwise, the generation is increased to the next generation for the target vector $\vec{X}_i^{g+1}$ and the algorithm is maintained. This case can be expressed as

$$\vec{X}_i^{g+1} = \begin{cases} \vec{u}_i^g, & e\breve{g}er \ f\left(\vec{u}_i^g\right) \leq f\left(\vec{X}_i^g\right) \\ \vec{X}_i^g, & e\breve{g}er \ f\left(\vec{u}_i^g\right) > f\left(\vec{X}_i^g\right) \end{cases} \tag{22}$$

5. Numerical Example

To demonstrate the effectiveness of the suggested methods with respect to reducing the cantilever beam's response, an analysis was carried out on the optimal design of TMDs. Previous studies have provided a beam model [16] that has six finite elements, where the length of each element is L = 1 m. This cantilever beam–TMD model with six nodes is depicted in Figure 3. There are two degrees of freedom at each node, which are vertical and rotational, and the single TMD is positioned at the 6th node of the cantilever beam. The lumped mass that is present at the 6th node is 100 kg. Section A is 0.05 m^2, the moment of inertia I is 2.08×10^4 m^4, the modulus of elasticity E is 2.06×10^{11} N/m^2, the shear modulus G is 7.94×10^{10} N/m^2, the shear correction factor κ is 3, and the mass density ρ is 7.8×10^3 kg/m^3. For the foremost modes of vibration, the natural damping ratio is $\xi_1 = \xi_2 = \xi_3 = 0.02$ for the first, second, and third modes, and it is considered that the damping matrix is proportional to the mass. The initial three modal natural frequencies

of the beam are $\omega_1 = 29.87$ rad/s, $\omega_2 = 187$ rad/s, and $\omega_3 = 526.31$ rad/s. The disturbance for design can be determined by considering the PSD function $S_{dist}(\omega)$ of the constant acceleration $\ddot{x}_{dist}$ for base excitation as a white noise within the given frequency range. This study considers PSD as $S_{dist}(\omega) = 0.015$ m^2/s^3, and the frequency range is described for the first mode control as 0.2 rad/s $\leq \omega \leq$ 60 rad/s, for the second mode control as 150 rad/s $\leq \omega \leq$ 200 rad/s, and the third mode control as 450 rad/s $\leq \omega \leq$ 650 rad/s.
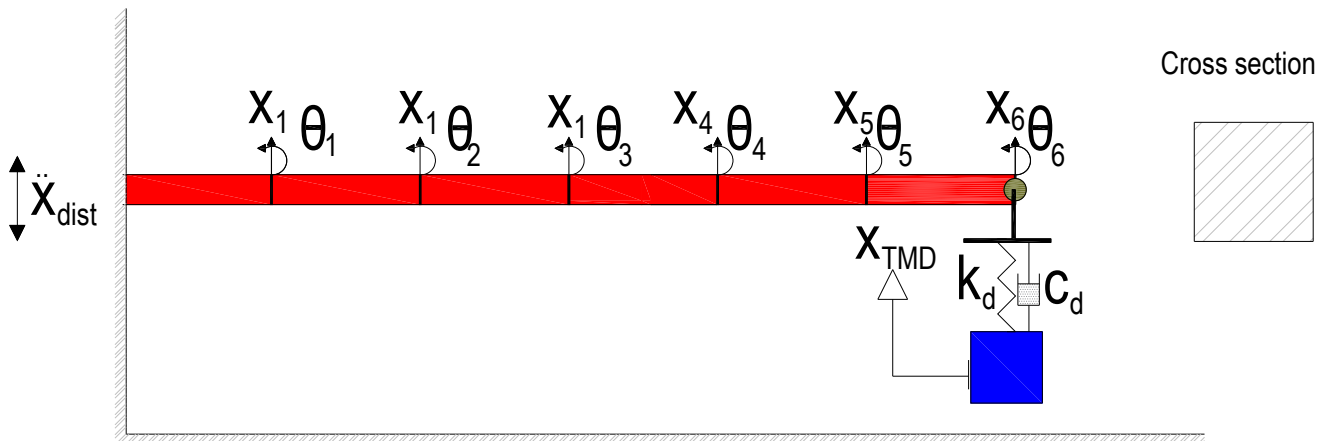
Figure 3. Cantilever beam–TMD model with six nodes.

To determine the optimum TMD parameters, i.e., stiffness, damping and mass coefficients, the objective function is taken to be the mean square of the absolute accelerations (f_1) and the mean square of the absolute displacement (f_2) which are to be decreased in the frequency domain. The DE algorithm is employed under the given constraints in this minimization process. The constraints are as follows for the stiffness, mass, and damping coefficients: $0 \leq \bar{k} \leq 4 \times 10^4$ N/m, $0 \leq \bar{m} \leq 20$ kg, and $0 \leq \bar{c} \leq 4 \times 10^3$ Ns/m for the first mode control, $0 \leq \bar{k} \leq 4 \times 10^6$ N/m, $0 \leq \bar{m} \leq 20$ kg, $0 \leq \bar{c} \leq 4 \times 10^5$ Ns/m for the second mode control and $0 \leq \bar{k} \leq 8 \times 10^6$ N/m, $0 \leq \bar{m} \leq 20$ kg, and $0 \leq \bar{c} \leq 8 \times 10^5$ Ns/m for the third mode control, respectively. Figure 4 demonstrates the variation in the transfer functions with respect to the design steps of the DE algorithm considering the first, second, and third modes of the beam with respect to f_1 and f_2 minimization. In this figure, it is evident that the objective function reaches a minimum value through design steps.

Considering all mode controls, the stiffness coefficient of TMD is the largest for the third mode control, then the second, and then the first. Figure 5 shows the frequency response of the sixth node's vertical absolute value of the absolute acceleration transfer function $|H_{AA6}(\omega)|$, absolute displacement transfer functions $|H_{D6}(\omega)|$, and sixth node rotation transfer function $|H_{R6}(\omega)|$ for f_1 and f_2 minimization of the first mode control. As seen in Figure 5, the TMD is successfully decreased for all responses of transfer functions. All results of the f_1 and f_2 objective functions give close response reductions, even though they differ.

To demonstrate the effectiveness of the TMD design the unit harmonic sinus functions of acceleration considering the first three natural frequencies and white noise base excitation, which has unit standard deviation and zero mean, are used at the cantilever beam as the base excitation. The harmonic excitations have frequencies equal to the first mode natural frequencies of the cantilever beam, ω_1, ω_2, and ω_3, so that the analyses can be performed under unfavorable conditions. All disturbance excitations are applied for 10 s durations, and are shown in Figure 6. In addition, the proposed method has been compared to some basic techniques, which are Warburton [29] and Sadek et al. [30], to show the advantages of the proposed method.
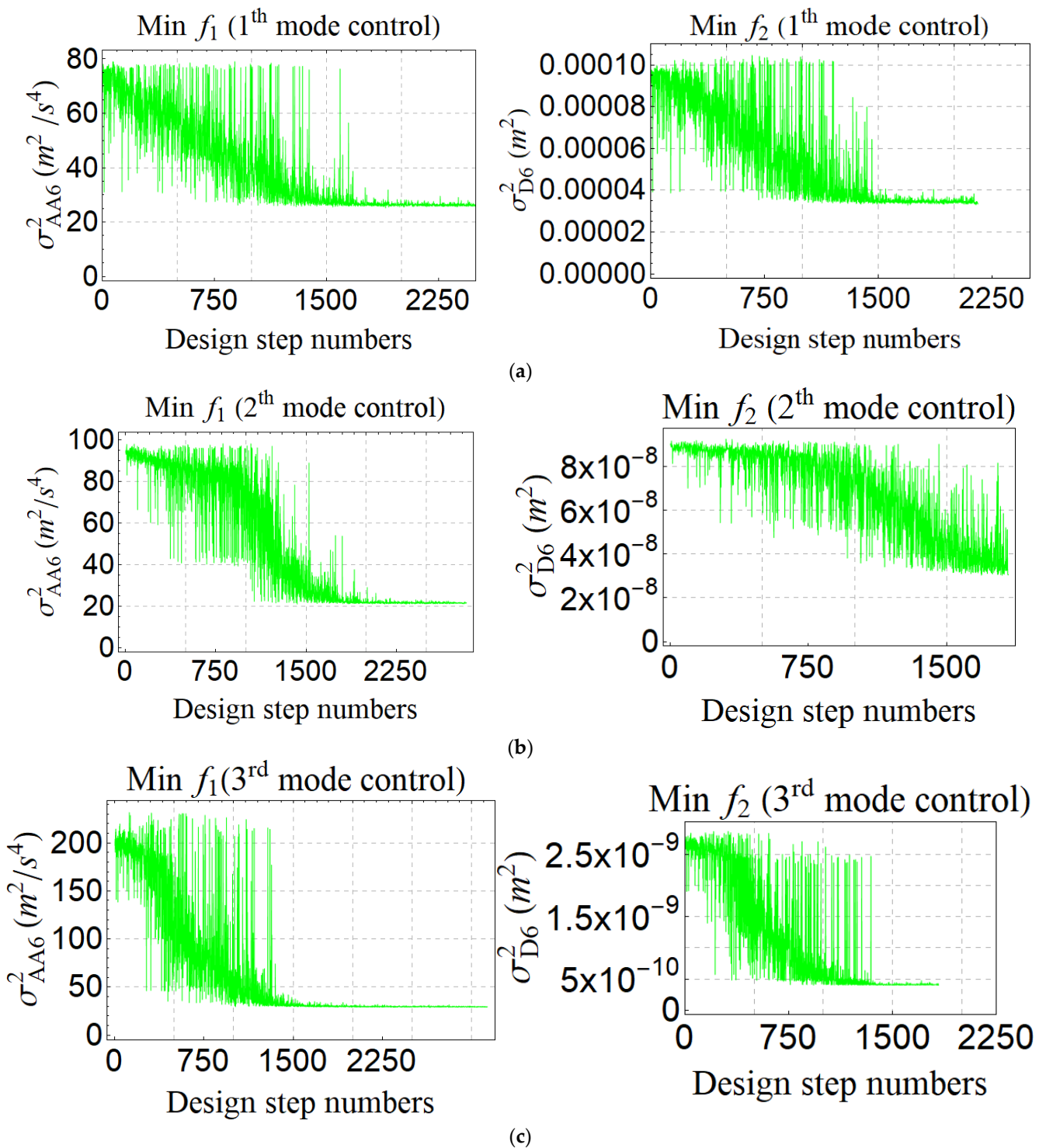
Figure 4. Variation in the transfer functions with respect to the design steps of the DE algorithm considering: (**a**) first, (**b**) second, and (**c**) third modes of the beam with respect to to f_1 and f_2 minimization.

Figure 5. Frequency response of: (**a**) 6th node vertical absolute acceleration transfer function $|H_{AA6}(\omega)|$, (**b**) absolute displacement transfer functions $|H_{D6}(\omega)|$, and (**c**) 6th node absolute rotational transfer function $|H_{R6}(\omega)|$ for f_1 and f_2 minimization of the first mode control.

1 Sin(ω_1)

(a)

1 Sin(ω_2)

(b)

Figure 6. *Cont.*

1 Sin(ω_3)

(c)

White noise excitation

(d)
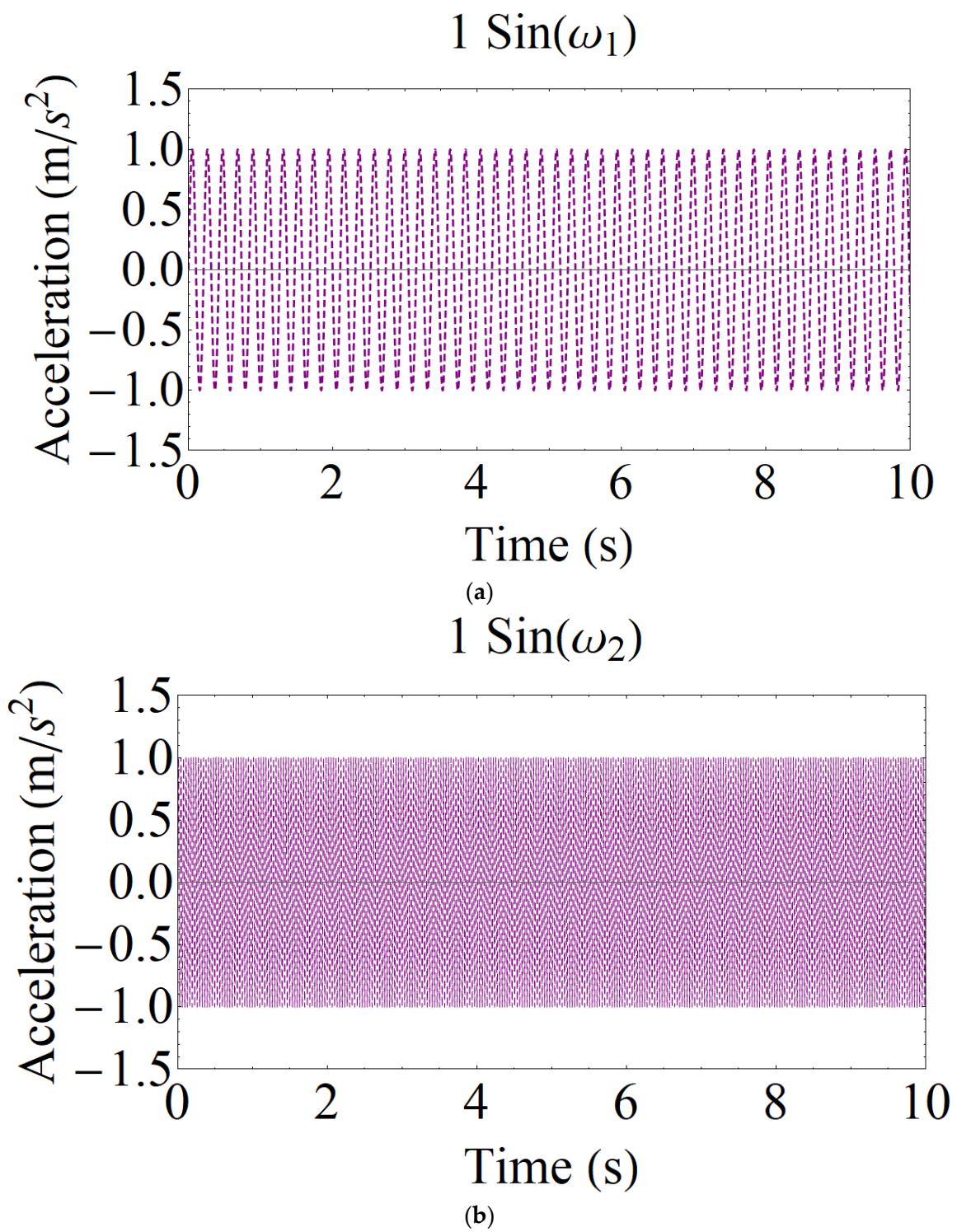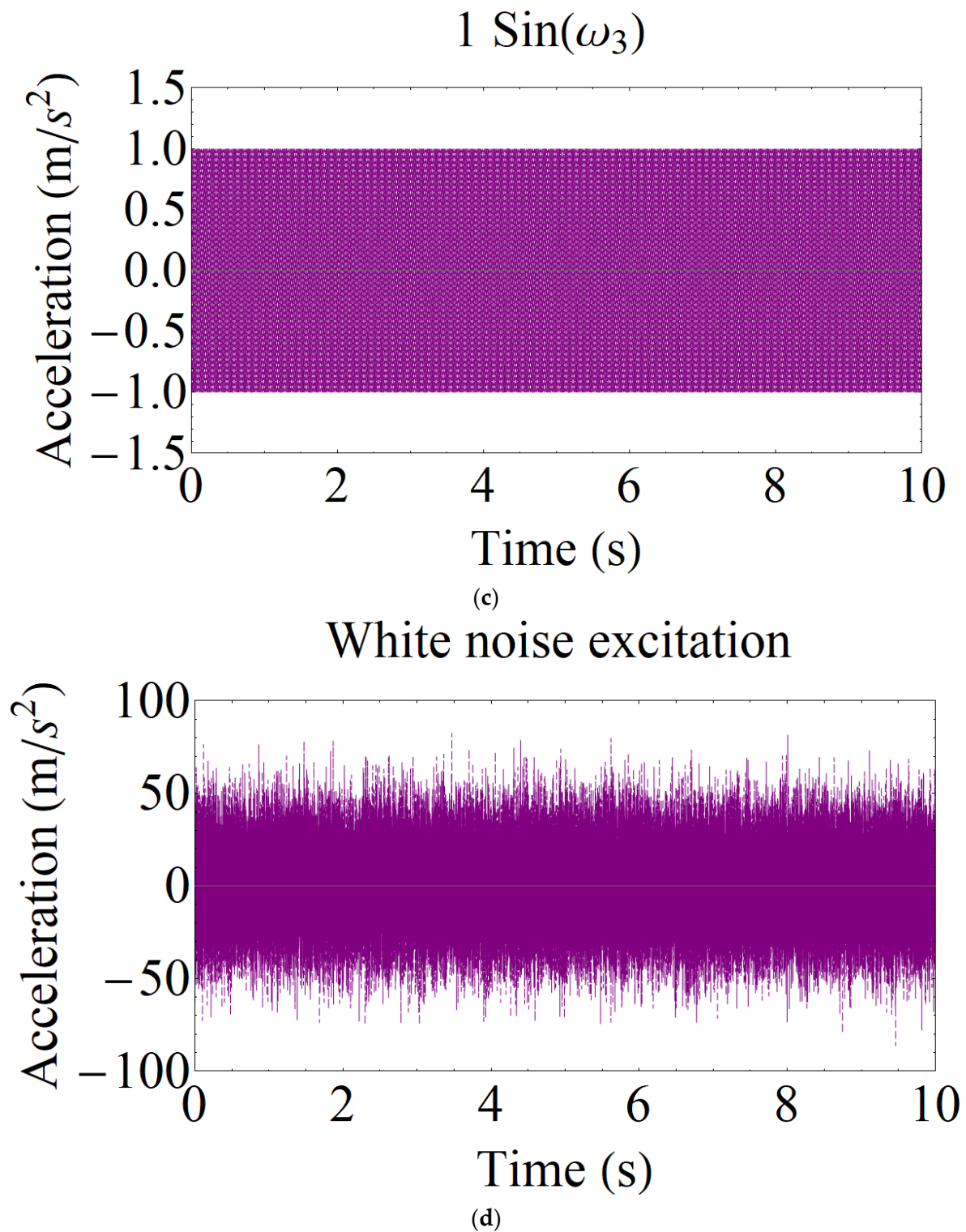
Figure 6. Disturbance base excitations: (**a**) 1 sin $\omega_1 t$, (**b**) 1 sin $\omega_2 t$, (**c**) 1 sin $\omega_3 t$, and (**d**) white noise excitation.

The method used by Warburton [23] to determine the optimum TMD parameters is based on white noise excitation. The formulation of the mass ratio μ_i for the ith mode, optimal tuning frequency f_{opt}, and damping ratio ξ_{dopt} can be specified as follows:

$$\mu_i = \frac{m_d}{\phi_i^T M_s \phi_i} \tag{23}$$

$$f_{opt} = \frac{\omega_d}{\omega_s} = \frac{1}{1+\mu}\sqrt{1-\mu/2} \tag{24}$$

$$\zeta_{dopt} = \sqrt{\frac{\mu(1-\mu/4)}{4(1+\mu)(1-\mu/2)}} \tag{25}$$

where $\boldsymbol{M}_s$ mass matrices of the structure, ω_{si} is the ith mode frequency of the structure, ω_d is the TMD frequency, and m_d is the mass of the TMD.

Sadek et al. [30] established a different optimization strategy for TMD design for MDOF systems. The tuning parameters can be expressed as follows:

$$f_{opt} = \frac{1}{1+\mu_i\phi_{ij}}(1 - \xi_i\sqrt{\frac{c\phi_{ij}}{1+\mu_i\phi_{ij}}}) \tag{26}$$

$$\zeta_{opt} = \phi_{ij}(\frac{\xi_i}{1+\mu_i} + \sqrt{\frac{\mu_i}{1+\mu_i}}) \tag{27}$$

In the above equation, ϕ_{ij} is the floor TMD location at the jth floor unit participation factor for the ith vibration mode amplitude. The structural damping ratio of the ith mode is indicated by ξ_i.

k_d (N/m) m_d (kg) c_d (Ns/m) describes the optimal TMD parameters, which are TMD stiffness, mass, and damping coefficients, respectively. Table 1 shows the optimum TMD parameters with respect to the present study's min f_1 and min f_2 and the methods of Warburton [29] and Sadek et al. [30] for the first, second, and third mode control of the cantilever beam.

Table 1. Optimal TMD parameters designed for cantilever beam.

TMD Parameters	Present Study Min f_1 (1 st Mode Control)	Present Study Min f_2 (1 st Mode Control)	Present Study Min f_1 (2 nd Mode Control)	Present Study Min f_2 (2 nd Mode Control)	Present Study Min f_1 (3 rd Mode Control)	Present Study Min f_2 (3 rd Mode Control)	Warburton [29] (1 st Mode Control)	Warburton [29] (2 nd Mode Control)	Warburton [29] (3 rd Mode Control)	Sadek et al. [30] (1 st Mode Control)	Sadek et al. [30] (2 nd Mode Control)	Sadek et al. [30] (3 rd Mode Control)
k_d (N/m)	17,159.16	16,563.27	695,738.21	666,785.85	5,541,584.86	5,360,683.44	17,770	670,488.11	4,854,157.53	17,755.86	631,566.79	4,474,847.14
m_d (kg)	19.84	20	20	20	20	19.85	20	20	20	20	20	20
c_d (Ns/m)	107.26	88.34	331.30	432.13	1400.73	854.88	25.69	529.95	2242.40	75.13	1052.54	4268.29

Figures 7–10 demonstrate the time history response of the vertical displacement, rotation, and acceleration of the sixth node of the cantilever beam under the harmonic base excitations for the first, second, and third modes and the white noise excitation considering the f_1 and f_2 objective functions. It can be seen in these figures that TMD is able to effectively decrease the displacement and acceleration reactions of the sixth node cantilever beam in a translational as well as rotational manner, with the harmonic base excitations being $1\sin\omega_1 t$, $1\sin\omega_2 t$, $1\sin\omega_3 t$, and the random unit white noise excitation. As seen in the figures, the TMD is more effective with respect to the reduction of harmonic load responses than white noise excitation, especially for the acceleration response.

The f_1 and f_2 objective functions are optimized according to the proposed method, and the peak displacement, peak rotation, and peak acceleration responses of the cantilever beam for the first, second, and third mode controls are compared with other methods [28,29]. These comparisons are shown in Table 2 and Figures 11–14. As observed in Figures 11–14, when the TMD is optimally designed with respect to the first and second mode resonance frequency, it remarkably decreases the effect of harmonic excitation with respect to the response of peak displacement, peak rotation, and peak acceleration for the f_1, f_2 objective functions methods of Warburton [29] and Sadek et al. [30]. However, even if the proposed method is partially successful in reducing the response of the cantilever beam, the methods of Warburton [29] and Sadek et al. [30] have a negative contribution to the response of the beam. As can be seen in Figure 14, considering random white noise excitation, f_1 and f_2 minimization in the proposed method and compared methods in literature [28,29] are also successful for response reductions except for peak acceleration. Classical solutions for TMD

design have concentrated on determining only the stiffness and damping parameters of the TMD. In the proposed method, mass optimization of TMD is also carried out. Additionally, while the classical solution of TMD is only efficient for one mode of control to reduce the structure's response, the proposed method for TMD design is efficient for more than one mode of control to reduce the cantilever beam's response.
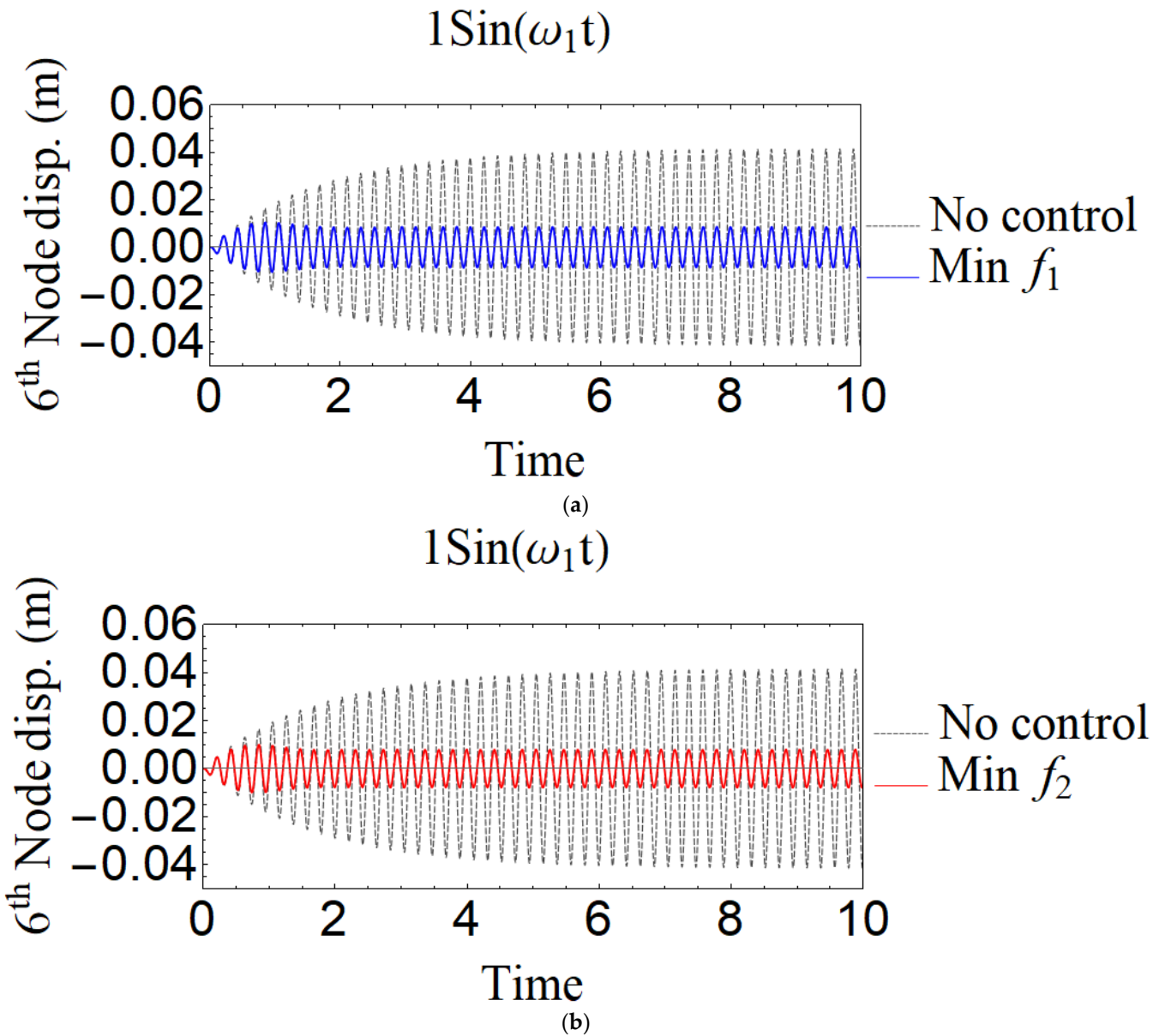
Figure 7. Time history response of the vertical displacement of the 6th node of the cantilever beam under the first mode harmonic base excitation considering (**a**) f_1 and (**b**) f_2 objective functions.
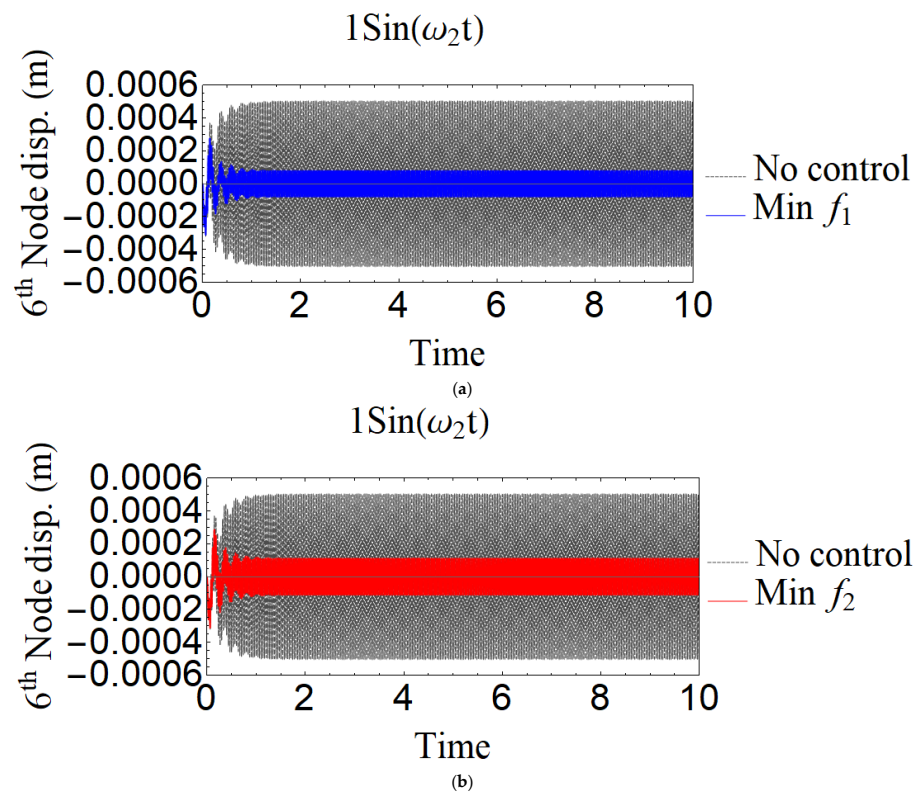
Figure 8. Time history response of the vertical displacement of the 6th node of the cantilever beam under the second mode harmonic base excitation considering (**a**) f_1 and (**b**) f_2 objective functions.
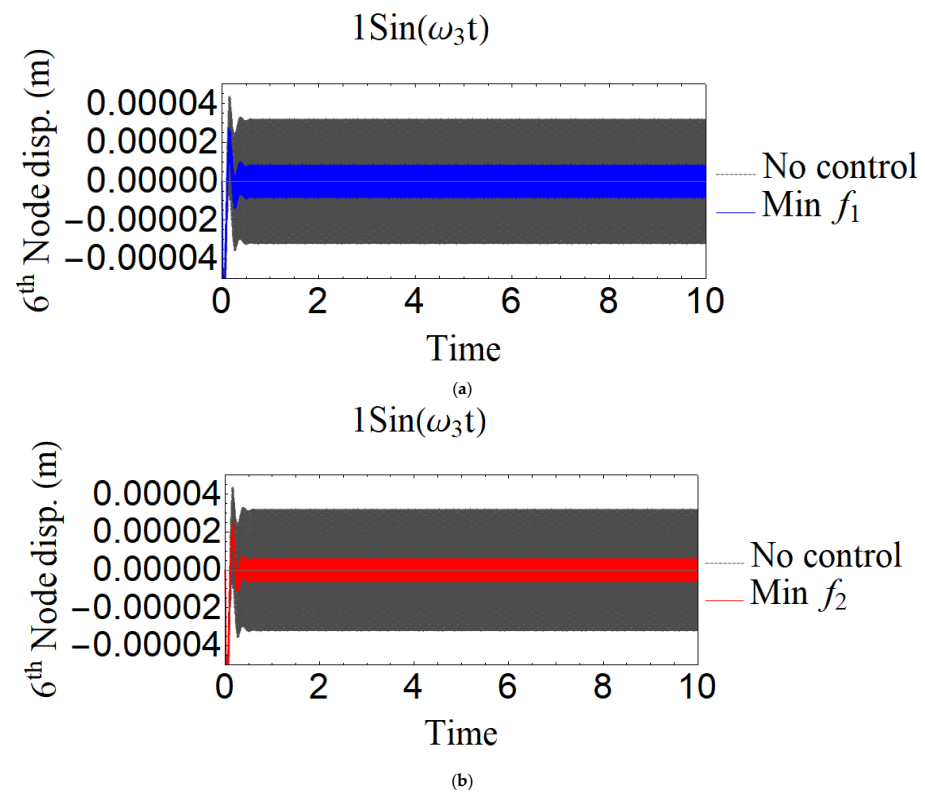
Figure 9. Time history response of the vertical displacement of the 6th node of the cantilever beam under the third mode harmonic base excitation considering (**a**) f_1 and (**b**) f_2 objective functions.
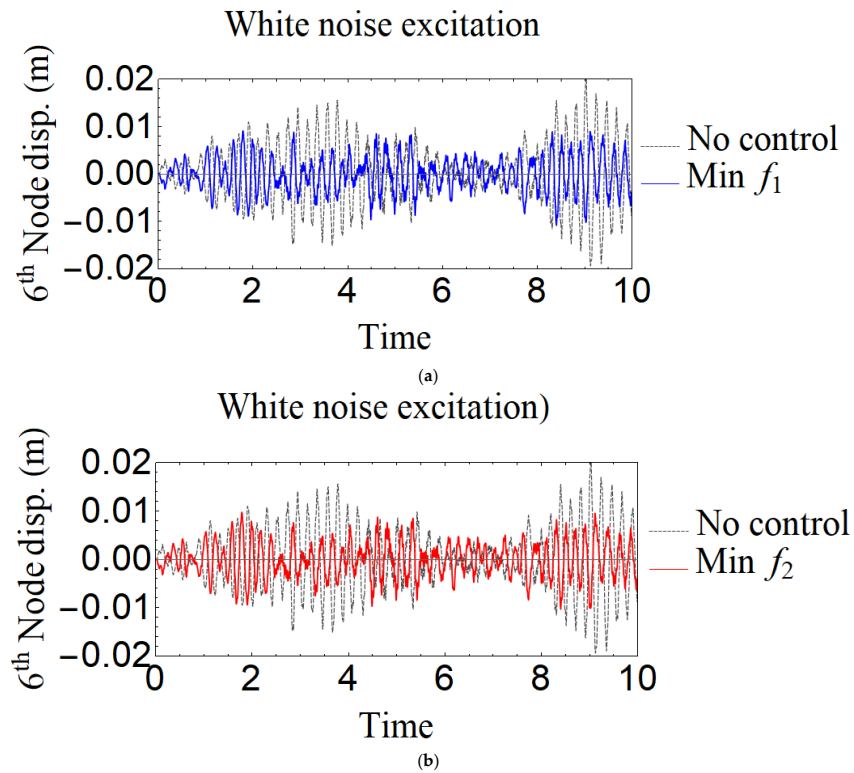
Figure 10. Time history response of the vertical displacement of the 6th node of the cantilever beam under the white noise base excitation considering (**a**) f_1 and (**b**) f_2 objective functions.

Figure 11. *Cont.*

(c)
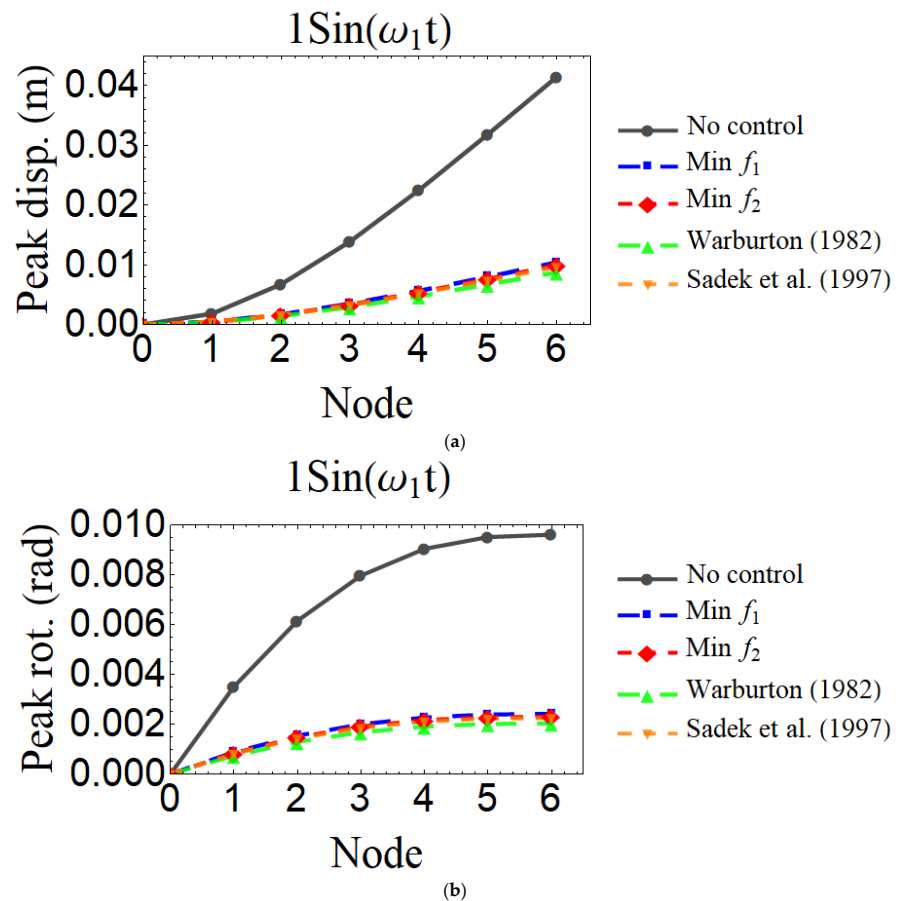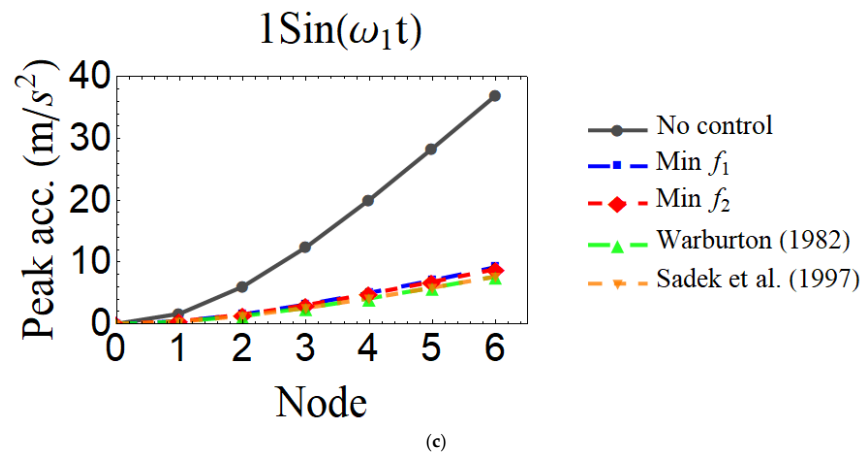
Figure 11. The peak node responses of the cantilever beam in comparison with [29,30] for the first mode control considering(**a**) peak displacements, (**b**) peak rotations, and (**c**) peak accelerations.

(a)

(b)

(c)
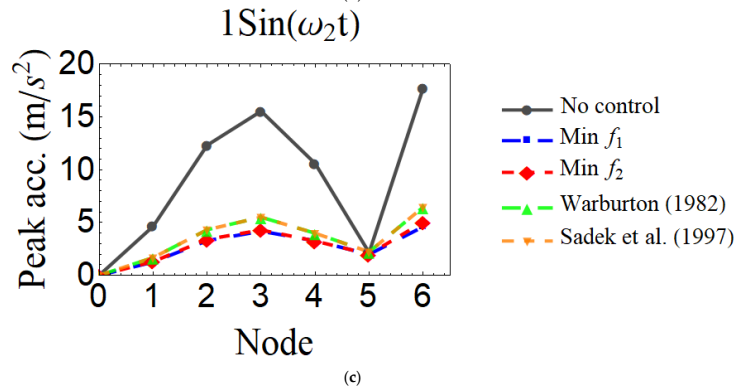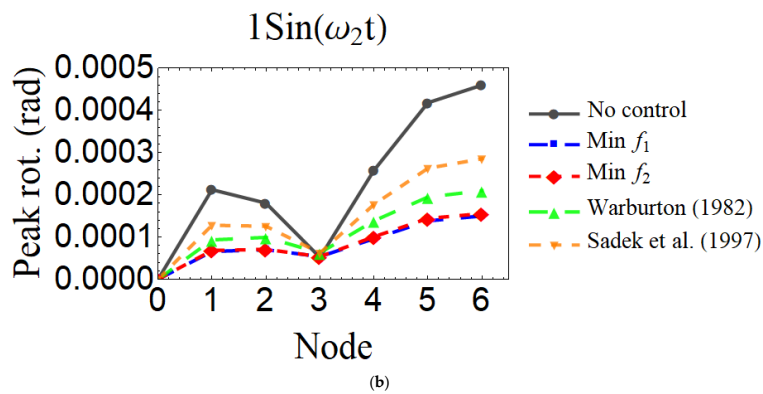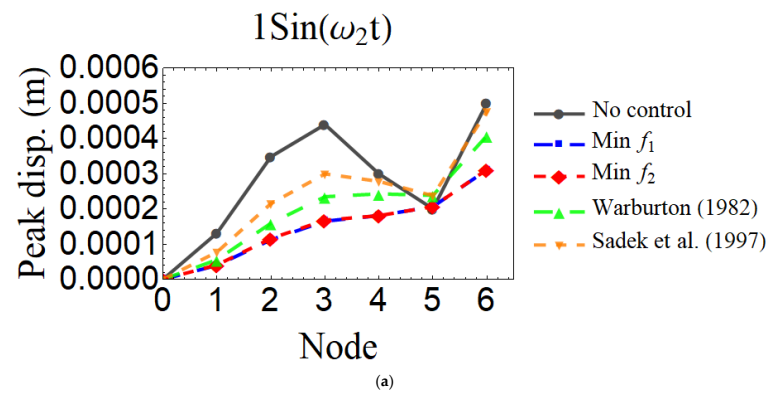
Figure 12. The peak node responses of the cantilever beam in comparison with [29,30] for the second mode control (**a**) peak displacements, (**b**) peak rotations, and (**c**) peak accelerations.
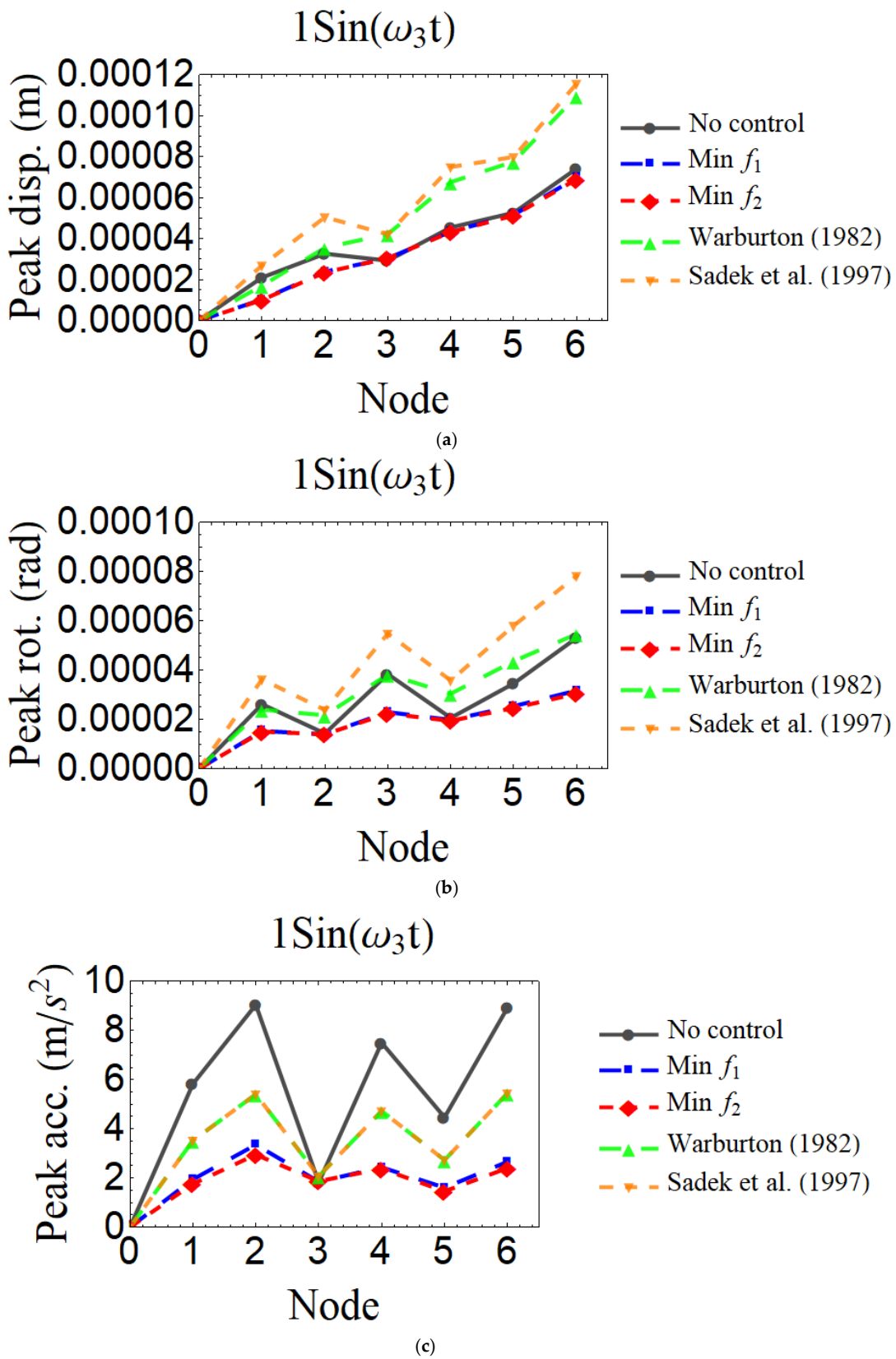
Figure 13. The peak node responses of the cantilever beam in comparison with [29,30] for the third mode control considering the f_1 and f_2 objective functions: (**a**) peak displacements, (**b**) peak rotations, and (**c**) peak accelerations.
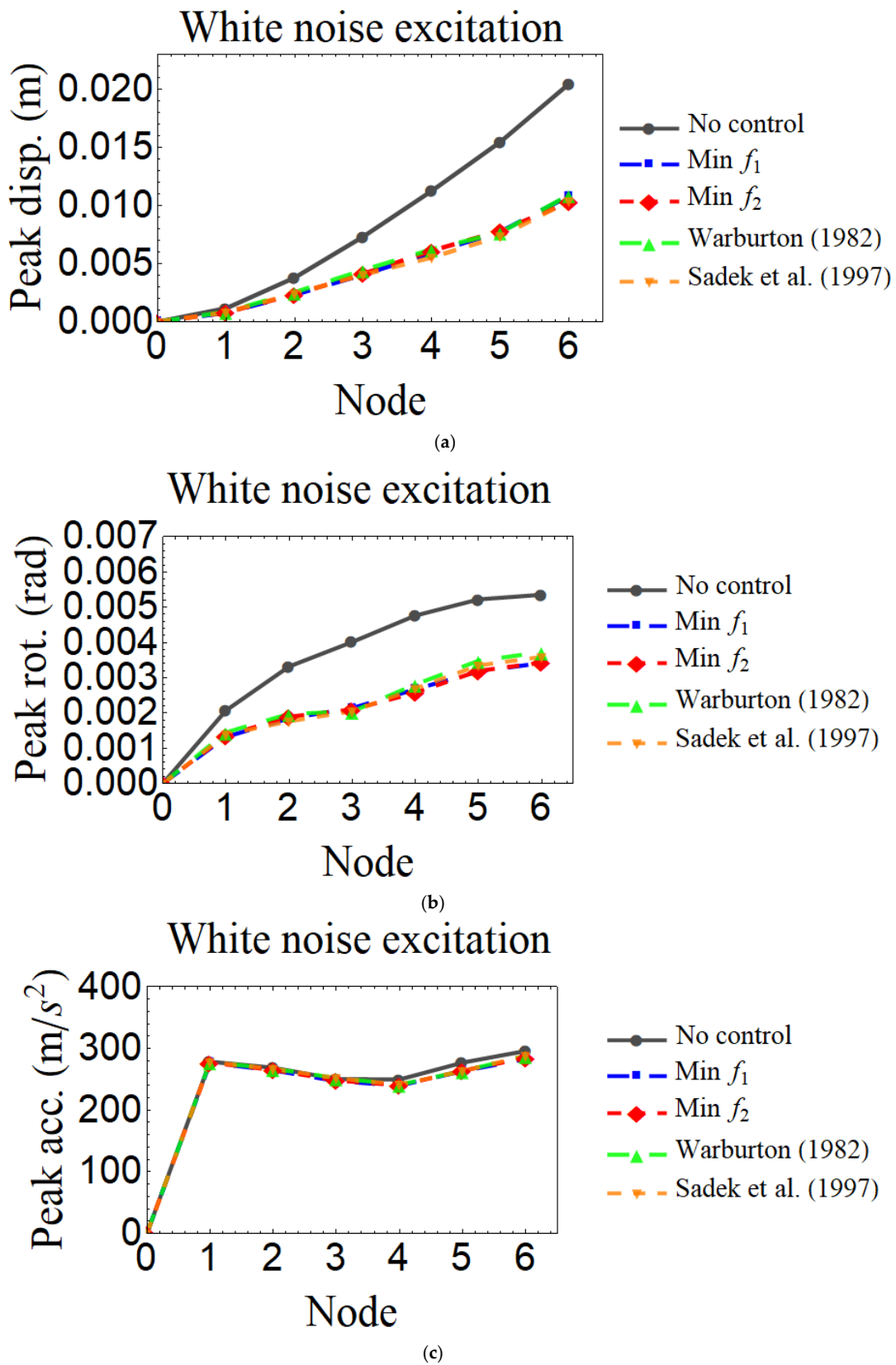
Figure 14. The peak node responses of the cantilever beam in comparison with [29,30] to the white noise excitation considering f_1 and f_2 objective functions: (**a**) peak displacements, (**b**) peak rotations, and (**c**) peak accelerations.

Table 2. In compression of 6th peak node responses of the cantilever beam for the first mode control considering peak displacements, rotations, and peak accelerations.

	Response	No	Min f_1		Min f_2		Warburton [29]		Sadek et al. [30]	
		Control	Value	Reduction (%)	Value	Reduction (%)	Value	Reduction (%)	Value	Reduction (%)
1 Sin ω_1	Peak displacement (m)	0.042	0.01	76.190	0.0099	76.429	0.0093	77.857	0.0097	76.905
	Peak rotation (rad)	0.0096	0.0024	75.000	0.0023	76.042	0.0022	77.083	0.0023	76.042
	Peak acceleration (m/s²)	36.99	9.18	75.182	8.86	76.048	7.7	79.184	8.5	77.021
1 Sin ω_2	Peak displacement (m)	0.0005	0.00031	38.000	0.00031	38.000	0.00041	18.000	0.00048	4.000
	Peak rotation (rad)	0.00046	0.00015	67.391	0.00016	65.217	0.00021	54.348	0.00029	36.957
	Peak acceleration (m/s²)	17.72	4.6	74.041	5.04	71.558	6.46	63.544	9.6	45.824
1 Sin ω_3	Peak displacement (m)	0.000074	0.00007	5.405	0.000069	6.757	0.00011	−48.649	0.00011	−48.649
	Peak rotation (rad)	0.000053	0.000032	39.623	0.00003	43.396	0.000055	−3.774	0.000078	−47.170
	Peak acceleration (m/s²)	8.93	2.66	70.213	2.4	73.124	5.45	38.970	9.61	7.615
White noise excitation	Peak displacement (m)	0.02	0.011	45.00	0.01	50.000	0.011	45.000	0.01	50.000
	Peak rotation (rad)	0.0053	0.0034	35.849	0.0034	35.849	0.0037	30.189	0.0036	32.075
	Peak acceleration (m/s²)	296	282.97	4.402	285.1	3.682	288.39	2.571	284.82	3.777

In the sixth node of the cantilever beam, considering the f_1 and f_2 minimization for the first mode control, the contour plots of the vertical absolute value of acceleration, displacement, rotation of the transfer functions $|H_{AA6}(\omega)|$, $|H_{D6}(\omega)|$, $|H_{R6}(\omega)|$ with respect to frequency and optimal mass, stiffness and damping coefficients of TMD are shown in Figures 15–17. In these figures, while a transfer function according to one of the TMD parameter (i.e., stiffness coefficient) and the excitation frequency is plotted, the optimal values of the other TMD parameters are stable. As it can be seen in the contour plots, when the mass, stiffness, and damping coefficients of TMD have their optimum values in resonance zone, the transfer function reaches a minimum value (optimum point).
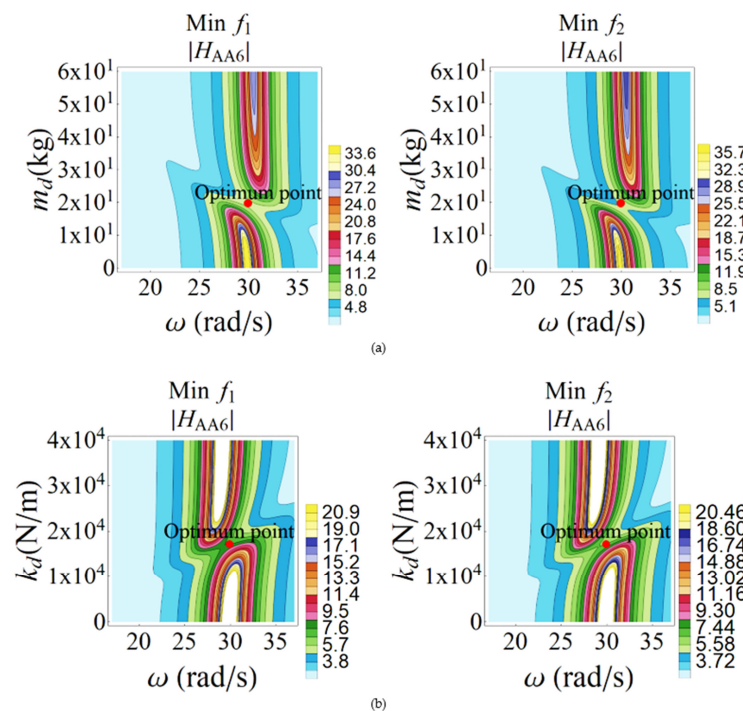
Figure 15. *Cont.*
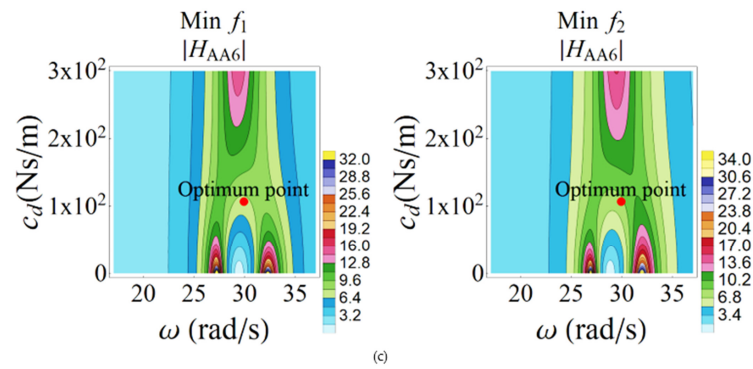
Figure 15. Contour plot of the 6th node vertical absolute acceleration transfer function $|H_{AA6}(\omega)|$ with respect to frequency and (**a**) TMD mass coefficient, (**b**) TMD stiffness coefficient, and (**c**) TMD damping coefficient, considering f_1 and f_2 minimization for the first mode control.
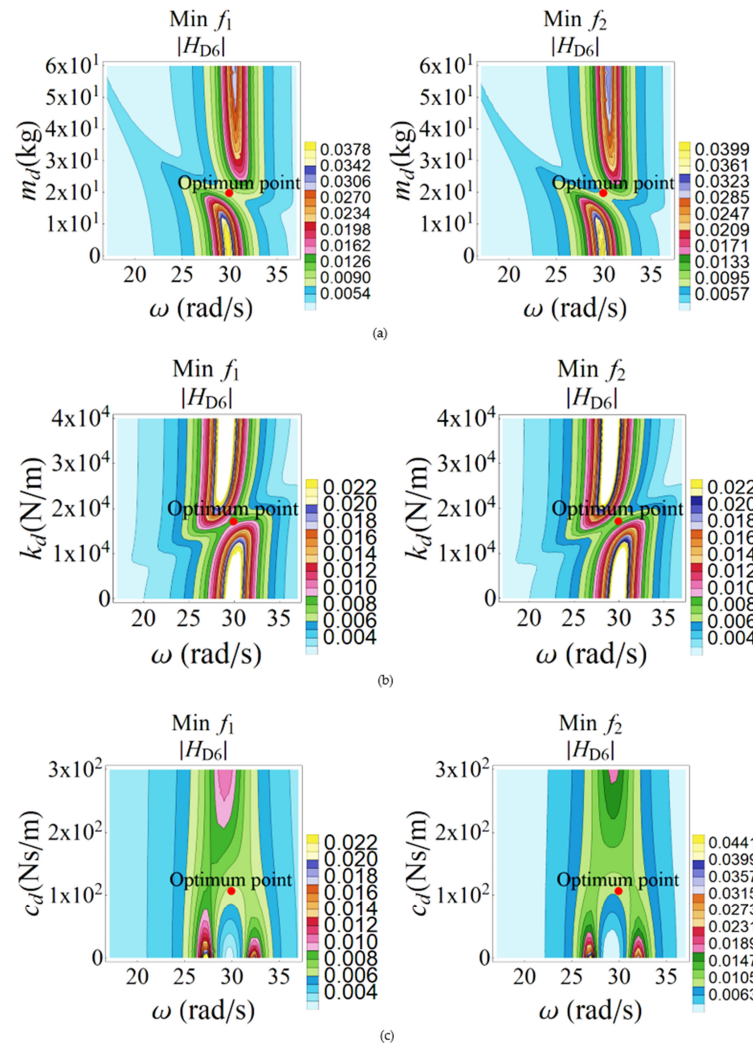
Figure 16. Contour plot of the 6th node vertical absolute displacement transfer function $|H_{D6}(\omega)|$, with respect to frequency and (**a**) TMD mass coefficient, (**b**) TMD stiffness coefficient, and (**c**) TMD damping coefficient, considering f_1 and f_2 minimization for the first mode control.
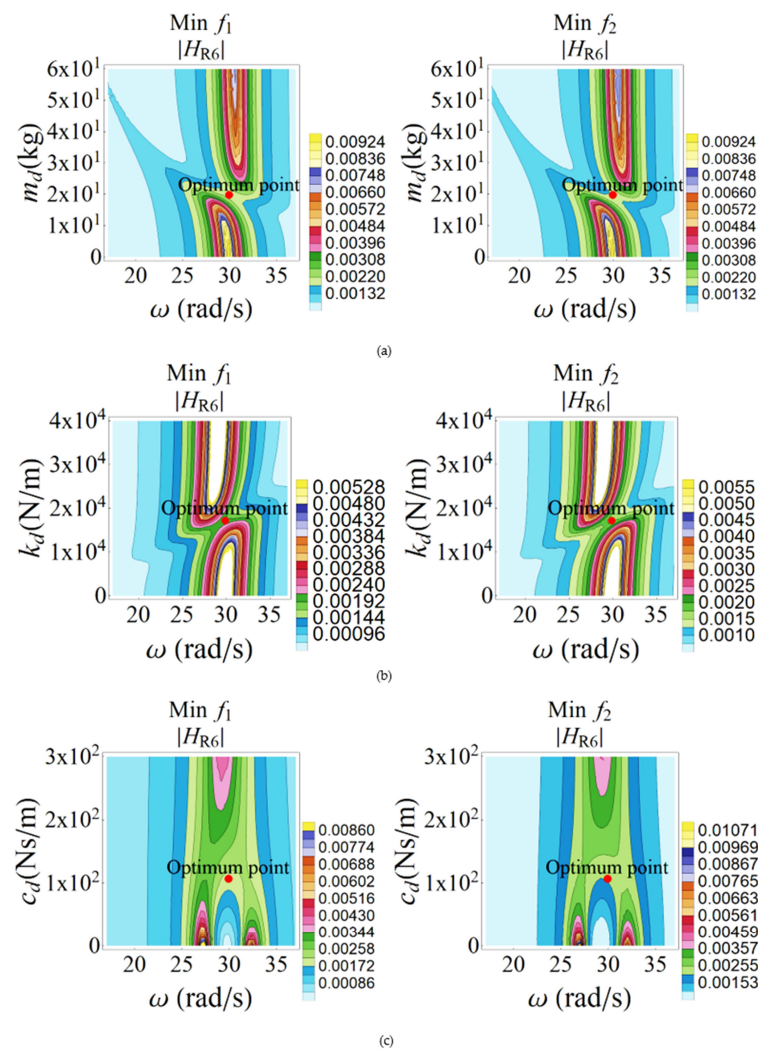
Figure 17. Contour plot of the 6th node rotation absolute transfer function $|H_{R6}(\omega)|$, with respect to frequency and (**a**) TMD mass coefficient, (**b**) TMD stiffness coefficient, and (**c**) TMD damping coefficient considering f_1 and f_2 minimization for the first mode control.

6. Conclusions

An optimal TMD design for the response reduction of a cantilever beam is examined in this study within the frequency domain. In addition to the stiffness and damping coefficients of the TMD, there is also optimization of the mass coefficients. The DE algorithm is used in this optimization by considering the constraints to determine the ideal parameters. The performance of the optimum designed TMD can be tested by exposing the cantilever beam–TMD system to a sinusoidal unit harmonic base excitation at the first, second, and third mode natural frequencies of the beam and white noise excitation. The conclusions derived from this study are listed below:

The properly calculated TMD dampers have been found to be quite successful in decreasing the transfer function of acceleration, displacement, and rotation reduction.

Even though TMD parameters are very different from each other, all results for the f_1 and f_2 objective functions provide an effective performance in reducing transfer functions, harmonic and white noise excitation responses.

The TMD is able to effectively decrease the displacement and acceleration reactions of the cantilever beam in a translational as well as rotational manner with the harmonic base excitations and the random unit white noise excitation. However, it is seen that TMD is not very effective in decreasing the white noise excitation for the acceleration response. It is also observed that TMD is more effective with respect to the reduction of harmonic

load responses than white noise excitation, especially for the acceleration response. The translational and rotational responses of cantilever beams can be effectively decreased by optimally developed TMDs with harmonic base excitations and their peak values.

The objective function that this study has employed is successful in appropriately developing the TMDs for response reduction.

The objective function in the frequency domain has been successfully minimized using the DE method.

When the TMD mass, stiffness, and damping coefficients reach an optimum value in the resonance zone, the transfer function convergences to minimum values.

The aim of future investigations is to study optimal design and distribution of multiple tuned mass dampers for cantilever beam response reduction.

References

1. Bernuzzi, C.; Crespi, P.; Montuori, P.; Nastri, E.; Simoncelli, M.; Stochino, F.; Zucca, M. Resonance of Steel Wind Turbines: Problems and Solution. *Structures* **2021**, *32*, 65–75. [CrossRef]
2. Soong, T.T.; Dargush, G.F. *Passive Energy Dissipation Systems in Structural Engineering*; John Wiley& Sons: Chichester, UK; New York, NY, USA, 1997.
3. Rana, R.; Soong T., T. Parametric study and simplified design of tuned mass dampers. *Eng. Struct.* **1998**, *20*, 193–204. [CrossRef]
4. Ormondroyd, J.; Den Hartog, J.P. The theory of dynamic vibration absorber. *Appl. Mech.* **1928**, *7*, 9–22.
5. Bishop, R.E.D.; Welbourn, D.B. The problem of the dynamic vibration absorber. *Engineering* **1952**, *174*, 769.
6. Falcon, K.C.; Stone, B.J.; Simcock, W.D.; Andrew, C. Optimization of vibration absorbers: A graphical method for use on idealized systems with restricted damping. *J. Mech. Eng. Sci.* **1967**, *9*, 374–381. [CrossRef]
7. Ioi, T.; Ikeda, K. On the dynamic vibration damped absorber of the vibration system. *Bull. JSME* **1978**, *21*, 64–71. [CrossRef]
8. Warburton, G.B.; Ayorinde, E.O. Optimum absorber parameters for simple systems. *Earthq. Eng. Struct. Dyn.* **1980**, *8*, 197–217. [CrossRef]
9. Vickery, B.J.; Isyumov, N.; Davenport, A.G. The role of damping. *MTMD Accel. J. Wind. Eng. Ind. Aerodyn* **1983**, *11*, 285–294. [CrossRef]
10. Villaverde, R.; Koyama, L.A. Damped resonant appendages to increase inherent damping in buildings. *Earthq. Eng. Struct. Dyn* **1993**, *22*, 491–507. [CrossRef]
11. Soto-Brito, R.; Ruiz, S.E. Influence of ground motion intensity on the effectiveness of tuned mass dampers. *Earthq. Eng. Struct. Dyn.* **1999**, *28*, 1255–1271. [CrossRef]
12. Bekdas, G.; Nigdeli, S.M. Estimating optimum parameters of tuned mass dampers using harmony search. *Eng. Struct.* **2011**, *33*, 2716–2723. [CrossRef]
13. Bekdas, G.; Nigdeli, S.M. Mass ratio factor for optimum tuned mass damper strategies. *Int. J. Mech. Sci.* **2013**, *71*, 68–84. [CrossRef]
14. Cetin, H.; Aydin, E.; Ozturk, B. Optimal damper allocation in shear buildings with tuned mass dampers and viscous dampers. *Int. J. Impact Eng.* **2017**, *2*, 89–120. [CrossRef]
15. Cetin, H.; Aydin, E. A New Tuned Mass Damper Design Method based on Transfer Functions. *KSCE J. Civ. Eng.* **2019**, *23*, 4463–4480. [CrossRef]
16. Takewaki, I. Optimal damper positioning in beams for minimum dynamic compliance. *Comput. Methods Appl. Mech. Engrg.* **1998**, *156*, 373. [CrossRef]
17. Wong, W.O.; Tang, S.L.; Cheung, Y.L.; Cheng, L. Design of a dynamic vibration absorber for vibration isolation of beams under point or distributed loading. *J. Sound Vib.* **2007**, *301*, 898–908. [CrossRef]

18. Bae, J.S.; Hwang, J.H.; Roh, J.H.; Yi, M.S.; Lim, J.H. Vibration suppression of a cantilever beam using magnetically tuned massdamper. *J. Sound Vib.* **2012**, *331*, 5669–5684. [CrossRef]

19. Aly, A.M. Proposed robust tuned mass damper for response mitigation in buildings exposed to multidirectional wind. *Struct. Des. Tall Spec. Build.* **2014**, *23*, 664–691. [CrossRef]

20. Zhang, M.; Xu, F. Tuned mass damper for self-excited vibration control: Optimization involving non-linear aeroelastic effect. *J. Wind. Eng. Ind. Aerodyn.* **2022**, *220*, 104836. [CrossRef]

21. Takewaki, I. *Building Control with Passive Dampers: Optimal Performance-Based Design for Earth-Quakes*; John Wiley & Sons: Hoboken, NJ, USA, 2009.

22. Przemieniecki, J.S. *Theory of Matrix Structural Analysis*; McGraw-Hill: New York, NY, USA, 1968.

23. Champion, B.; Strzebonski, A. *Constrained optimization, Wolfram Mathematica Tutorial Collection*; Wolfram Research, Inc.: Long Hanborough, UK, 2008.

24. Storn, R.; Price, K.V. Differential evolution a simple and efficient heuristic for global optimization over continuous spaces. *J. Global Optim.* **1997**, *11*, 341–359. [CrossRef]

25. Penunuri, F.; Escalante, R.P.; Villanueva, C.; Oy, D.P. Synthesis of mechanisms for single and hybrid tasks using differential evolution. *Mech. Mach. Theory* **2011**, *46*, 1335–1349. [CrossRef]

26. Wu, G.; Shen, X.; Li, H.; Chen, H.; Lin, A.; Suganthan, P.N. Ensemble of differential evolution variants. *Inf. Sci.* **2018**, *423*, 172–186. [CrossRef]

27. Biswas, P.P.; Suganthan, P.N.; Wu, G.; Amaratunga, G.A.J. Parameter estimation of solar cells using datasheet information with the application of an adaptive differential evolution algorithm. *Renew. Energy* **2019**, *132*, 425–438. [CrossRef]

28. Ronkkonen, J.; Kukkonen, S.; Price, K.V. Ronkkonen J, Kukkonen S, Price KV. Real-parameter optimization with differential evolution. In Proceedings of the 2005 IEEE Congress on Evolutionary Computation, Edinburgh, UK, 2–5 September 2005; Volume 1, pp. 506–513.

29. Warburton, G.B. Optimal absorber parameters for various combinations of response and excitation parameters. *Earthq. Eng. Struct. Dyn.* **1982**, *10*, 381–401. [CrossRef]

30. Sadek, F.; Mohraz, B.; Taylor, A.W.; Chung, R.M.A. Method of estimating the parameters of tuned mass dampers for seismic applications. *Earthq. Eng. Struct. Dyn.* **1997**, *26*, 617–635. [CrossRef]